Estimation of Synchronization Parameters in AF Cooperative Networks

Ali A. Nasir,[1] Hani Mehrpouyan,[2] Steven D. Blostein,[3] Salman Durrani,[1] and Rodney A. Kennedy[1]

[1]Research School of Engineering, CECS, The Australian National University, Canberra, Australia.
[2]Department of Signals and Systems, Chalmers University of Technology, Sweden.
[3]Department of Electrical and Computer Engineering, Queen's University, Kingston, Canada.
Emails: ali.nasir@anu.edu.au, hani.mehr@ieee.org, steven.blostein@queensu.ca, salman.durrani@anu.edu.au, rodney.kennedy@anu.edu.au

***Abstract*—In cooperative networks, multiple carrier frequency offsets (MCFOs) and multiple timing offsets (MTOs) originate due to multiple distributed nodes. In this paper, algorithms for joint estimation of these parameters and channels in amplify-and-forward (AF) relaying networks are proposed. A new training model and transceiver structure at the relays for achieving synchronization throughout the network is devised. New exact closed-form expressions for the *Cramér-Rao lower bounds* (CRLBs) for the multi-parameter estimation problem are derived. An estimation method is proposed for jointly estimating MCFOs, MTOs, and channel gains at the destination based on *space-alternating generalized expectation maximization (SAGE)* and compared to a computationally-intensive *least squares (LS)* approach. The proposed estimator's performance is shown to be close to the CRLB at mid-to-high signal-to-noise ratio (SNR) resulting in significant cooperative performance gains in the presence of practical impairments.**

I. Introduction

Cooperative communications is an attractive low cost solution to combat fading in wireless systems, where multiple single antenna terminals cooperatively transmit their received signals to a designated node [1]. As a result, cooperative communication can be an attractive approach for meeting the higher throughput demands by the future wireless systems. However, in cooperative systems, the application of multiple distributed nodes, each with their own local oscillator, gives rise to MTOs and MFCOs [2], [3].

Cramér-Rao lower bounds (CRLB) and different techniques for estimating MTOs and MCFOs in decode-and-forward (DF) and amplify-and-forward (AF) cooperative systems are derived in [3]–[6] and [2], respectively. However, the analyses in [2]–[6] are focussed on estimating one set of system parameters while assuming that the remaining system parameters are perfectly estimated and compensated, e.g., estimating MTOs while assuming perfect frequency synchronization [3], [5], [6] or vice versa [2], [4]. However, such an idealistic assumption does not hold in practical cooperative systems, where the channel gains, MCFOs, and MTOs need to be jointly estimated. This fact is highlighted in [7], where joint maximum likelihood (ML) estimation of MCFOs, MTOs, and channels for DF cooperative systems is investigated. However, the ML estimator in [7] is very computationally complex. Joint channel estimation and time-frequency synchronization for uplink orthogonal frequency-division multiple access systems are proposed in [8], [9], that exploits the cyclic prefix. However, depending on the number of sub-carriers used, the frequency acquisition range of the algorithms in [8], [9] is very limited. To the best of the authors' knowledge, the problem of joint MCFOs, MTOs, and channel estimation with CRLB derivation for AF cooperative systems is not analyzed in any existing literature.

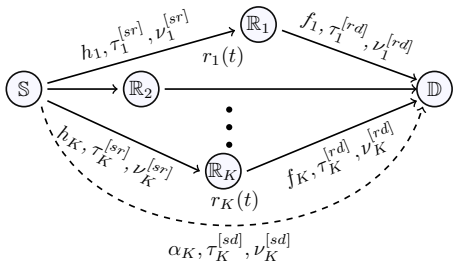

Fig. 1: The system model for the cooperative network.

In [10], we address estimation of MCFOs, MTOs, and channels in multi-relay cooperative networks. On the other hand, in this paper, we focus on AF relaying cooperative networks and present a new zero-forcing equalization scheme that allows for efficient equalization of MTOs, MCFOs, and channel gains in AF relaying cooperative networks. In addition, the performance of the proposed SAGE estimator for different number of relays, length of training sequences, and different network setups is investigated.

Notation: Superscripts $(\cdot)^*$ and $(\cdot)^T$ denote the conjugation and the transpose operators, respectively. Bold face small letters, e.g., $\mathbf{x}$, are used for vectors, bold face capital alphabets, e.g., $\mathbf{X}$, are used for matrix representation. $\mathbf{I}_X$ is used to denote the idenity matrix of size $X \times X$, $\odot$ stands for Schur (element-wise) product, $|\cdot|$ is the modulus operator and $\|\mathbf{x}\|$ represents the L_2 norm of a vector $\mathbf{x}$. $\mathbb{E}\{\cdot\}$ assumes the expected value of the corresponding sequence. $\Re\{\cdot\}$ and $\Im\{\cdot\}$ take the real and imaginary parts of a complex quantity. diag$(\mathbf{X})$ is used to denote the diagonal elements of the matrix $\mathbf{X}$, mod(a/b) finds the remainder of division of a by b, and $\lfloor\cdot\rfloor$ indicates the floor function.

II. System Model and Training Algorithm

We consider a half-duplex space division multiple access single-input-single-output (SISO) cooperative system with one source node, $\mathbb{S}$, K relays, $\mathbb{R}_1, \cdots, \mathbb{R}_K$, and a single destination node, $\mathbb{D}$ (Fig. 1). Quasi-static and frequency flat-fading channels are considered, which is motivated by prior research in this field in [2]–[6]. The channel gains from $\mathbb{S}$ to $\mathbb{R}_k$, $\mathbb{R}_k$ to $\mathbb{D}$, and $\mathbb{S}$-$\mathbb{R}_k$-$\mathbb{D}$ are denoted by h_k, f_k, and α_k, respectively, for $k = \{1, \cdots, K\}$. In Fig. 1, τ_k and ν_k are used to denote timing offsets and CFOs, where superscripts, $(\cdot)^{[sr]}$, $(\cdot)^{[rd]}$ and $(\cdot)^{[sd]}$ denote offsets from $\mathbb{S}$ to $\mathbb{R}_k$, $\mathbb{R}_k$ to $\mathbb{D}$, and $\mathbb{S}$ to $\mathbb{D}$, respectively. Transmission of signals from source to relays to destination consists of a *training period* (TP) as well as a *data transmission period* (DTP). Without loss of generality, it is assumed that during the TP, unit-amplitude phase shift keying (PSK) training signals (TSs) are transmitted to $\mathbb{D}$.

978-1-4577-2053-6/12/$31.00 ©2012 IEEE

A. Relay Processing

The block diagram for the proposed AF transceiver at $\mathbb{R}_k$ and AF receiver at $\mathbb{D}$ are depicted in Figs. 2 and 3, respectively. The received signal at $\mathbb{R}_k$ is down converted by oscillator frequency, $\omega_k^{[r]}$, and then over sampled by the factor Q. The sampled received signal at the input of timing estimation block, $r_k(i)$ is given by[1]

$$r_k(i) = h_k \sum_{n=0}^{L-1} t^{[s]}(n) g\left(iT_s - nT - \tau_k^{[sr]}T\right) e^{j2\pi i \nu_k^{[sr]}/Q} + u_k(i), \tag{1}$$

where $\nu_k^{[sr]}$ is the CFO, normalized by the symbol duration T, between $\mathbb{S}$ and $\mathbb{R}_k$, h_k denotes the *unknown* channel gain from $\mathbb{S}$ to $\mathbb{R}_k$ that is assumed to be static over a frame but distributed as $\mathcal{CN}(0, \sigma_h^2)$ from frame to frame, $\tau_k^{[sr]}$ is the fractional unknown timing offset, normalized by T, between $\mathbb{S}$ and $\mathbb{R}_k$, T_s is the sampling time period such that $T_s = T/Q$, $g(t)$ is the transmitter pulse shaping function, L is the length of the TS, $t^{[s]}(n)$, and $u_k(i)$ is the zero-mean complex baseband additive white Gaussian noise (AWGN) at $\mathbb{R}_k$ with variance $\sigma_{u_k}^2$, i.e., $u_k(i) \sim \mathcal{CN}(0, \sigma_{u_k}^2)$. It is assumed that the noise at all relays have the same variance, i.e., $\sigma_u^2 = \sigma_{u_1}^2 = \cdots = \sigma_{u_K}^2$.

In order to ensure synchronous transmission and successful cooperation for AF networks, a timing detector at the k^{th} relay estimates the corresponding timing offset, $\hat{\tau}_k^{[sr]}$, using schemes available for point-to-point SISO systems as outlined in [11]. The timing offset estimate $\hat{\tau}_k^{[sr]}$ is used as an input to the complex analog multiplier to ensure that the k^{th} relay's unit amplitude training signal, $\bar{t}_k^{[r]}(t)$, is multiplied by the received signal $r_k(t)$ at the appropriate time. The training signal used here is given by $t_k^{[r]}(t) = e^{-j\phi_k(n)}$ for $(n-1)T < t < nT$, where $\phi_k(n)$ is in between $(-\pi, \pi)$ and denotes the phase of the n^{th} symbol of the k^{th} relay's training signal, where $\phi_k(n) \neq \phi_{\bar{k}}(n)$, for $k \neq \bar{k}$. The output of the multiplier, $s_k(t)$, is given by

$$s_k(t) = t_k^{[r]}(t) h_k e^{j2\pi F_k^{[sr]} t} \sum_{n=0}^{L-1} g\left(t - nT - \epsilon_k^{[sr]}T\right) \times t^{[s]}(n) + t_k^{[r]}(t) u_k(t), \tag{2}$$

where $\epsilon_k^{[sr]} = \tau_k^{[sr]} - \hat{\tau}_k^{[sr]}$ is timing estimation error and $F_k^{[sr]} = \nu_k^{[sr]}/T$ is the analog frequency offset between $\mathbb{S}$ and $\mathbb{R}_k$.

Remark 1: Unlike [3], the proposed processing structure at the relays in Fig. 2 does not assume perfect timing and frequency offset estimation and matched-filtering at the relays. Moreover, in our proposed model, the relays do not perform frequency offset and channel estimation during the TP.

B. Destination Processing

The received signal at $\mathbb{D}$, $\mathbf{y} \triangleq [y(0), \cdots, y(QL-1)]^T$, is given by

$$\mathbf{y} = \mathbf{\Omega}\boldsymbol{\alpha} + \mathbf{\Psi}\boldsymbol{\beta} + \mathbf{w}, \tag{3}$$

where:

- $\mathbf{\Omega} \triangleq \left[(\mathbf{\Lambda}_1 \mathbf{G}_1 \mathbf{t}^{[s]}) \odot \mathbf{t}_1^{[r]}(\tau_k^{[rd]}), \cdots, (\mathbf{\Lambda}_K \mathbf{G}_K \mathbf{t}^{[s]}) \odot \mathbf{t}_K^{[r]}(\tau_k^{[rd]})\right]$,
- $\mathbf{\Lambda}_k \triangleq \text{diag}\left(\left[e^{j2\pi\nu_k^{[sd]}(0)/Q}, \cdots, e^{j2\pi\nu_k^{[sd]}(QL-1)/Q}\right]\right)$,
- $[\mathbf{G}_k]_{m,\ell} \triangleq g\left(mT_s - \ell T - \tau_k^{[sd]}T\right)$ is a $QL \times L$ matrix,

[1]For clarity, we reserve the index $n = \{0, \cdots, L-1\}$ for T-spaced samples and index $i = \{0, \cdots, QL-1\}$ for T_s-spaced samples.

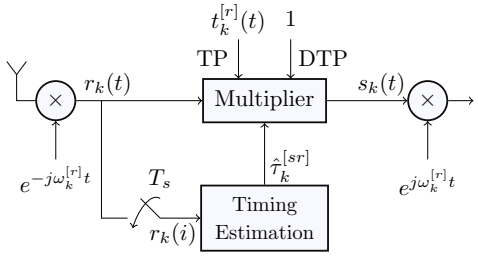

Fig. 2: Block Diagram for the proposed AF k^{th} Relay Transceiver.

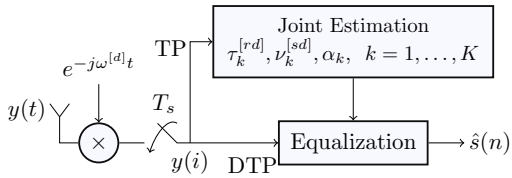

Fig. 3: Block Diagram for the proposed AF Destination Receiver.

- $\tau_k^{[sd]} \triangleq \tau_k^{[rd]} + \epsilon_k^{[sr]}$,[2] $\tau_k^{[rd]}$ is the timing offset between $\mathbb{R}_k$ and $\mathbb{D}$,
- $\mathbf{\Psi} \triangleq \left[\bar{\mathbf{\Lambda}}_1 \mathbf{v}_1, \cdots, \bar{\mathbf{\Lambda}}_K \mathbf{v}_K\right]$,
- $\bar{\mathbf{\Lambda}}_k \triangleq \text{diag}\left(\left[e^{j2\pi\nu_k^{[rd]}(0)/Q}, \cdots, e^{j2\pi\nu_k^{[rd]}(QL-1)/Q}\right]\right)$,
- $\nu_k^{[rd]}$ is the normalized CFO from $\mathbb{R}_k$ to $\mathbb{D}$, $\nu_k^{[sd]} \triangleq \nu_k^{[sr]} + \nu_k^{[rd]}$ is the sum of CFOs from $\mathbb{S}$–$\mathbb{R}_k$–$\mathbb{D}$,
- $\mathbf{t}_k^{[r]}(\tau_k^{[rd]}) \triangleq \left[t_k^{[r]}(\tau_k^{[rd]}T), \cdots, t_k^{[r]}((QL-1)T_s - \tau_k^{[rd]}T)\right]^T$,
- $\mathbf{t}^{[s]} \triangleq \left[t^{[s]}(0), \cdots, t^{[s]}(L-1)\right]^T$,
- $\mathbf{w} \triangleq [w(0), \cdots, w(QL-1)]^T$, $\mathbf{v}_k \triangleq [v_k(0), \cdots, v_k(QL-1)]^T$, $w(i) \sim \mathcal{CN}(0, \sigma_w^2)$ is the AWGN at $\mathbb{D}$, $v_k(i) \triangleq u_k(i) t_k^{[r]}\left(iT_s - \tau_k^{[rd]}T\right)$, and
- $\boldsymbol{\alpha} \triangleq [\alpha_1, \cdots, \alpha_K]^T$, $\boldsymbol{\beta} \triangleq [\beta_1, \cdots, \beta_K]^T$, $\alpha_k \triangleq \zeta_k f_k h_k$, $\beta_k \triangleq \zeta_k f_k$, $f_k \sim \mathcal{CN}(0, \sigma_f^2)$ denotes the complex *unknown* channel gain from $\mathbb{R}_k$ to $\mathbb{D}$, $\zeta_k = 1/\sqrt{\sigma_h^2 + \sigma_u^2}$ satisfies the k^{th} relay's power constraint.

In (3) $u_k(i)$ has been used in place of $u_k(iT_s - \tau_k^{[rd]}T)$ since $u_k(t)$ denotes the AWGN and its statistics are not affected by the change in the sampling point. Note that $v_k(i)$ has the same statistical properties as $u_k(i)$ due to the assumption of unit-amplitude training signals.

At the destination, as shown in Fig 3, joint estimation of MCFOs, MTOs, and channel gains is performed and on the basis of those estimates, the received signal is equalized to detect the transmitted data symbols.

III. Cramer-Rao Lower Bound

In this section, new exact closed-form CRLBs for joint estimation of multiple channel gains, MCFOs, and MTOs for AF-relaying cooperative networks are derived. Given the signal model at $\mathbb{D}$ in (3), the parameter vector of interest $\boldsymbol{\theta}$, is given by

$$\boldsymbol{\theta} \triangleq \left[\Re\{\boldsymbol{\alpha}\}^T, \Im\{\boldsymbol{\alpha}\}^T, \boldsymbol{\nu}^T, \boldsymbol{\tau}^T\right]^T, \tag{4}$$

where $\boldsymbol{\nu} \triangleq [\nu_1, \cdots, \nu_K]^T$ and $\boldsymbol{\tau} \triangleq [\tau_1, \cdots, \tau_K]^T$ and for notational simplicity, ν_k and τ_k are used to denote $\nu_k^{[sd]}$ and $\tau_k^{[rd]}$, respectively.

[2]The signal model at destination takes into account the timing offset estimation error from $\mathbb{S}$-$\mathbb{R}$.

Based on the proposed training method, *Fisher's information matrix* (FIM) for the estimation of $\boldsymbol{\theta}$ is given in (5) at the bottom of this page, where $\sigma_n^2 \triangleq \sigma_u^2 \sum_{k=1}^{K} |\beta_k|^2 + \sigma_w^2$, $\boldsymbol{\Gamma} \triangleq [(\boldsymbol{\Lambda}_1 \mathbf{R}_1 \mathbf{t}^{[s]}) \odot \mathbf{t}_1^{[r]}(\tau_k^{[rd]}), \cdots, (\boldsymbol{\Lambda}_K \mathbf{R}_K \mathbf{t}^{[s]}) \odot \mathbf{t}_K^{[r]}(\tau_k^{[rd]})]$, $\mathbf{D} \triangleq 2\pi/Q \times \text{diag}\big([0, 1, \cdots, LQ-1]\big)$, $\mathbf{H} \triangleq \text{diag}(\alpha_1, \cdots, \alpha_K)$, and $\mathbf{R}_k \triangleq \partial \mathbf{G}_k / \partial \tau_k$ (Proof, see [10]).

Let us define $\mathbf{F}_{11}$ and $\mathbf{F}_{22}$ as the upper left and lower right $2K \times 2K$ sub matrices of $\mathbf{F}$, respectively, and $\mathbf{Z}$ as the upper right $2K \times 2K$ sub matrix of $\mathbf{F}$. Using the partitioned matrix inverse, the closed-form CRLB for the estimation of MCFOs, MTOs and multiple channel gains, $\boldsymbol{\alpha}$, can be written as

$$\mathbf{CRLB}(\boldsymbol{\nu}, \boldsymbol{\tau}) = \frac{\sigma_n^2}{2} \text{diag}\Big(\boldsymbol{\Upsilon}\Big), \tag{6}$$

$$\mathbf{CRLB}(\boldsymbol{\alpha}) = \frac{2}{\sigma_n^2} \text{diag}\Big(\mathbf{B}\mathbf{F}_{11}^{-1}\mathbf{B}^H + \mathbf{B}\mathbf{F}_{11}^{-1}\mathbf{Z}\boldsymbol{\Upsilon}\mathbf{Z}^T\mathbf{F}_{11}^{-1}\mathbf{B}^H\Big), \tag{7}$$

where $\mathbf{B} \equiv [\mathbf{I}_K \; j\mathbf{I}_K]$ is used to obtain the CRLB of $\boldsymbol{\alpha}$ from the CRLB of $\Re\{\boldsymbol{\alpha}\}$ and $\Im\{\boldsymbol{\alpha}\}$ according to [12], $\boldsymbol{\Upsilon} \triangleq \mathbf{F}_{22}^{-1} + \mathbf{F}_{22}^{-1}\mathbf{Z}^T(\mathbf{F}_{11} - \mathbf{Z}\mathbf{F}_{22}^{-1}\mathbf{Z}^T)^{-1}\mathbf{Z}\mathbf{F}_{22}^{-1}$,

$$\mathbf{F}_{11}^{-1} = \begin{bmatrix} \Re\{(\boldsymbol{\Omega}^H\boldsymbol{\Omega})^{-1}\} & -\Im\{(\boldsymbol{\Omega}^H\boldsymbol{\Omega})^{-1}\} \\ \Im\{(\boldsymbol{\Omega}^H\boldsymbol{\Omega})^{-1}\} & \Re\{(\boldsymbol{\Omega}^H\boldsymbol{\Omega})^{-1}\}, \end{bmatrix}, \tag{8}$$

and $\mathbf{F}_{22}^{-1}$ is given in (10) at the top of this page, where $\boldsymbol{\Phi}_{11} \triangleq \Re\{\mathbf{H}^H\boldsymbol{\Omega}^H\mathbf{D}^2\boldsymbol{\Omega}\mathbf{H}\}$, $\boldsymbol{\Phi}_{12} \triangleq \Im\{\mathbf{H}^H\boldsymbol{\Omega}^H\mathbf{D}\boldsymbol{\Gamma}\mathbf{H}\}$, $\boldsymbol{\Phi}_{21} = \boldsymbol{\Phi}_{21}^H$, and $\boldsymbol{\Phi}_{22} \triangleq \Re\{\mathbf{H}^H\boldsymbol{\Gamma}^H\boldsymbol{\Gamma}\mathbf{H}\}$. The following remark is in order:

Remark 2: Eqs. (5), (6), and (7) demonstrate that the FIM and the CRLB for the joint estimation of MCFOs, MTOs, and channel gains are not block diagonal. Thus, there exist coupling between the estimation errors of MCFOs, MTOs, and channel gains. This shows the importance of jointly estimating MCFOs, MTOs, and channel gains in multi-relay cooperative networks. More importantly, this result indicates that the previously proposed methods that assume perfect frequency or timing synchronization while estimating MCFOs and MTOs in [3] and [2], respectively, cannot be applied to estimate MCFOs, MTOs, and multiple channel gains jointly in distributed AF cooperative networks.

IV. Joint Parameter Estimation

In this section the LS and SAGE algorithms for joint estimation of MCFOs, MTOs, and multiple channel gains are derived and their computational complexity is analyzed.

A. LS Estimator

Based on the training signal model in (3), the LS estimate of $\boldsymbol{\alpha}, \boldsymbol{\nu}$, and $\boldsymbol{\tau}$ can be determined as

$$\hat{\boldsymbol{\alpha}} = (\boldsymbol{\Omega}^H\boldsymbol{\Omega})^{-1}\boldsymbol{\Omega}^H\mathbf{y}. \tag{10}$$

$$\hat{\boldsymbol{\nu}}, \hat{\boldsymbol{\tau}} = \arg\max_{\boldsymbol{\nu},\boldsymbol{\tau}} \mathbf{y}^H\boldsymbol{\Omega}(\boldsymbol{\Omega}^H\boldsymbol{\Omega})^{-1}\boldsymbol{\Omega}^H\mathbf{y}. \tag{11}$$

TABLE I: Proposed SAGE Algorithm.

Initialization

Obtain $\hat{\nu}_k^{[0]}, \hat{\tau}_k^{[0]}$, and $\hat{\alpha}_k^{[0]}$ for $k = 1, \ldots, K$ using alternating projection, (15) and (16) with coarser step size like 0.01

Iterative updates of the Estimation Parameters

for $m = 0, 1, \ldots$

for $k = 1, 2, \ldots, K$

$\hat{\mathbf{x}}_k^{[m]} = \mathbf{y} - \sum_{\ell=1, \ell\neq k}^{K} \hat{\alpha}_\ell^{[m]} \big(\hat{\boldsymbol{\Lambda}}_\ell^{[m]} \hat{\mathbf{G}}_\ell^{[m]} \mathbf{t}^{[s]}\big) \odot \mathbf{t}_\ell^{[r]}$

$\hat{\nu}_k^{[m+1]} = \hat{\nu}_k^{[m]} - \frac{\sum_{i=0}^{LQ-1} \big(\frac{2\pi i}{Q}\big) \Im\big\{p_k^{[m]}(i) e^{j2\pi i \hat{\nu}_k^{[m]}/Q} b_i\big(\hat{\tau}_k^{[m]}\big)\big\}}{\sum_{i=0}^{LQ-1} \big(\frac{2\pi i}{Q}\big)^2 \Re\big\{p_k^{[m]}(i) e^{j2\pi i \hat{\nu}_k^{[m]}/Q} b_i\big(\hat{\tau}_k^{[m]}\big)\big\}}$

$\hat{\tau}_k^{[m+1]} = \hat{\tau}_k^{[m]} - \frac{\sum_{i=0}^{LQ-1} \Re\big\{p_k^{[m]}(i) e^{j2\pi i \hat{\nu}_k^{[m+1]}/Q} b_i'\big(\hat{\tau}_k^{[m]}\big)\big\}}{\sum_{i=0}^{LQ-1} \Re\big\{p_k^{[m]}(i) e^{j2\pi i \hat{\nu}_k^{[m+1]}/Q} b_i''\big(\hat{\tau}_k^{[m]}\big)\big\}}$

$\hat{\alpha}_k^{[m+1]} = \frac{\sum_{i=0}^{LQ-1} \hat{x}_k^{[m]}(i) e^{-j2\pi i \hat{\nu}_k^{[m+1]}/Q} \big(t_k^{[r]}(i)\big)^* \big(b_i(\hat{\tau}_k^{[m+1]})\big)^*}{\sum_{i=0}^{LQ-1} |b_i(\hat{\tau}_k^{[m+1]})|^2 |t_k^{[r]}(i)|^2}$

end

$\hat{\nu}_k^{[m]} = \hat{\nu}_k^{[m+1]}$, $\hat{\tau}_k^{[m]} = \hat{\tau}_k^{[m+1]}$, $\hat{\alpha}_k^{[m]} = \hat{\alpha}_k^{[m+1]}$.

end

The maximization in (11) is carried out using *alternating projection* (AP) [3], [5] which reduces the multi-dimensional maximization problem into a series of one-dimensional searches [3], [5]. Note that in order to reach the CRLB for the estimation of MCFOs, MTOs, and channel gains (See Fig. 4 in Section V), the step size for the exhaustive search in (11) needs to be very small, e.g., 10^{-5}, which significantly increases the computational complexity of LS estimator. To reduce the computational cost of this exhaustive search, a SAGE estimator is derived below.

B. SAGE Estimator

The entries in the vector $\boldsymbol{\theta}$ in (4) are rearranged into the new parameter vector $\boldsymbol{\lambda} \triangleq \big[\boldsymbol{\lambda}_1^T, \cdots, \boldsymbol{\lambda}_K^T\big]^T$ in this section, where $\boldsymbol{\lambda}_k \triangleq [\nu_k, \tau_k, \alpha_k]^T$, for $k = \{1, \cdots, K\}$. The SAGE algorithm is an *expectation maximization* (EM) based iterative algorithm which updates the parameters sequentially by alternating among the subsets of parameters that make up the hidden data space[3]. Thus, using the SAGE algorithm, the parameter $\boldsymbol{\lambda}$ is divided into K groups denoted by $\boldsymbol{\lambda}_k$, for $k = \{1 \cdots, K\}$ [13]. During the estimation process, the estimates for each group of parameters are updated while the estimates for the remaining groups are fixed at their latest updated values. For each group, a *hidden data set* is selected [13]. In this case, the hidden data set denoted by $\mathbf{x}_k$ for $\boldsymbol{\lambda}_k$ is given by

$$\mathbf{x}_k = \alpha_k \big(\boldsymbol{\Lambda}_k \mathbf{G}_k \mathbf{t}^{[s]}\big) \odot \mathbf{t}_k^{[r]}(\tau_k^{[rd]}) + \mathbf{n}, \tag{12}$$

where $\mathbf{n} \triangleq \boldsymbol{\Psi}\boldsymbol{\beta} + \mathbf{w}$ is the overall noise vector in (3). The SAGE algorithm iteratively alternates between an *E-step*, calculating the conditional expectation of the hidden-data space log-likelihood,

[3]The SAGE algorithm is applied here since in [13] its shown that it converges more quickly than the EM or expectation conditional maximization algorithms.

$$\mathbf{F} = \frac{2}{\sigma_n^2} \begin{bmatrix} \Re\{\boldsymbol{\Omega}^H\boldsymbol{\Omega}\} & -\Im\{\boldsymbol{\Omega}^H\boldsymbol{\Omega}\} & -\Im\{\boldsymbol{\Omega}^H\mathbf{D}\boldsymbol{\Omega}\mathbf{H}\} & \Re\{\boldsymbol{\Omega}^H\boldsymbol{\Gamma}\mathbf{H}\} \\ \Im\{\boldsymbol{\Omega}^H\boldsymbol{\Omega}\} & \Re\{\boldsymbol{\Omega}^H\boldsymbol{\Omega}\} & \Re\{\boldsymbol{\Omega}^H\mathbf{D}\boldsymbol{\Omega}\mathbf{H}\} & \Im\{\boldsymbol{\Omega}^H\boldsymbol{\Gamma}\mathbf{H}\} \\ \Im\{\mathbf{H}^H\boldsymbol{\Omega}^H\mathbf{D}\boldsymbol{\Omega}\} & \Re\{\mathbf{H}^H\boldsymbol{\Omega}^H\mathbf{D}\boldsymbol{\Omega}\} & \Re\{\mathbf{H}^H\boldsymbol{\Omega}^H\mathbf{D}\mathbf{D}\boldsymbol{\Omega}\mathbf{H}\} & \Im\{\mathbf{H}^H\boldsymbol{\Omega}^H\mathbf{D}\boldsymbol{\Gamma}\mathbf{H}\} \\ \Re\{\mathbf{H}^H\boldsymbol{\Gamma}^H\boldsymbol{\Omega}\} & -\Im\{\mathbf{H}^H\boldsymbol{\Gamma}^H\boldsymbol{\Omega}\} & -\Im\{\mathbf{H}^H\boldsymbol{\Gamma}^H\mathbf{D}\boldsymbol{\Omega}\mathbf{H}\} & \Re\{\mathbf{H}^H\boldsymbol{\Gamma}^H\boldsymbol{\Gamma}\mathbf{H}\} \end{bmatrix} \tag{5}$$

$$\mathbf{F}_{22}^{-1} = \begin{bmatrix} (\boldsymbol{\Phi}_{11} - \boldsymbol{\Phi}_{12}\boldsymbol{\Phi}_{22}^{-1}\boldsymbol{\Phi}_{21})^{-1} & -\boldsymbol{\Phi}_{11}^{-1}\boldsymbol{\Phi}_{12}(\boldsymbol{\Phi}_{22} - \boldsymbol{\Phi}_{21}\boldsymbol{\Phi}_{11}^{-1}\boldsymbol{\Phi}_{12})^{-1} \\ -\boldsymbol{\Phi}_{22}^{-1}\boldsymbol{\Phi}_{21}(\boldsymbol{\Phi}_{11} - \boldsymbol{\Phi}_{12}\boldsymbol{\Phi}_{22}^{-1}\boldsymbol{\Phi}_{21})^{-1} & (\boldsymbol{\Phi}_{22} - \boldsymbol{\Phi}_{21}\boldsymbol{\Phi}_{11}^{-1}\boldsymbol{\Phi}_{12})^{-1} \end{bmatrix} \tag{10}$$

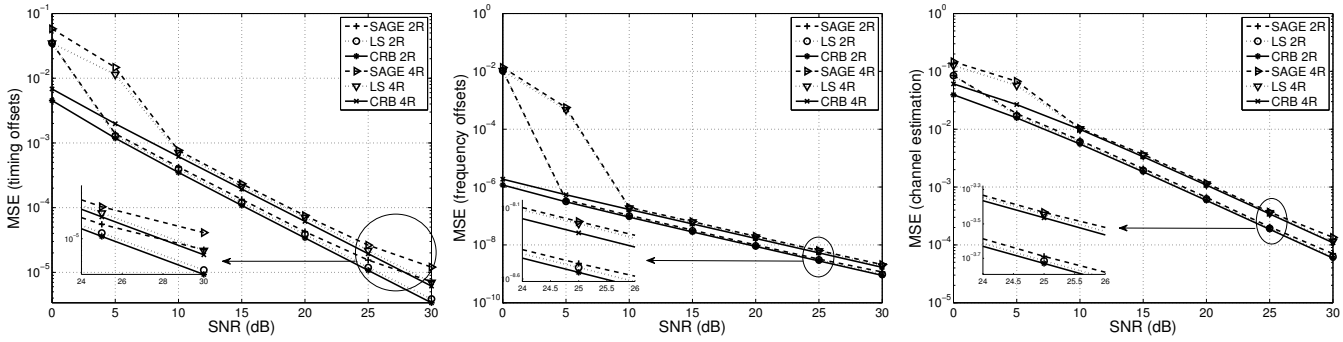

(a) (b) (c)

Fig. 4: MSE and CRLBs of (a) MTOs, (b) MCFOs and (c) channel coefficients estimation as a function of SNR (dB).

and an *M-step*, maximizing the expectation *with respect to* (w.r.t) unknown parameters. The SAGE estimator is summarized in Table I (Derivation, see [10]), where $p_k^{[m]}(i) = \left(\hat{x}_k^{[m]}(i)\right)^* \hat{\alpha}_k^{[m]} t_k^{[r]}(i)$, $b_i(\tau_k) = \sum_{\ell=-Lg}^{Lg} t^{[s]}(\ell + \lfloor i/Q \rfloor)\, g(\mathrm{mod}(i/Q)T_s - \ell T - \tau_k T)$, L_g is the selected pulse shaping filter lag in the TP, $b_i'(\tau_k)$ and $b_i''(\tau_k)$ are the first and second order derivatives of the function $b_i(\tau_k)$ w.r.t. τ_k and $\hat{\nu}_k^{[m]}$, $\hat{\tau}_k^{[m]}$ and $\hat{\alpha}_k^{[m]}$ denote the estimated values of ν_k, τ_k and α_k, respectively, at the m^{th} iteration. The iterative process is terminated when the difference between the *log-likelihood function* (LLF) of two iterations is smaller than $\chi = 0.001$.

Note that in [13, Page 4] it is shown that the SAGE algorithm monotonically increases the LLF at every iteration and converges to a local maximum. Moreover, if the algorithm is initialized in a region suitably close to the global maximum, the sequence of estimates converge monotonically to the global maximum [13, Page 4]. In our simulation, initial rough estimates, $\hat{\nu}_k^{[0]}, \hat{\tau}_k^{[0]}, \hat{f}_k^{[0]}$, are obtained using AP via (11) while using a coarse step size, e.g., 10^{-2}. Simulation results in Section V indicate that the proposed SAGE estimator converges to the true estimates with this initialization procedure. Compared to the LS estimator this significantly larger step size significantly reduces the computational complexity associated with the estimation process as shown next.

C. Complexity of the Proposed Estimators

The computational complexity of the proposed algorithms is evaluated using CPU execution time [14]. The execution time is observed at SNR = 20 dB with $K = 4$ relays, when an Intel Core 2 Quad 2.66 GHz processor with 4 GB of RAM is used. It has been observed that execution time for the proposed LS and SAGE estimators is 270 and 0.291 minutes respectively, which shows that compared to the LS estimator, the SAGE estimator is capable of estimating the desired parameters approximately 926 times more quickly.

V. Simulation Results

In this section, we present simulation results to evaluate the performance of our estimators. The propagation loss is modeled as $\eta = (d/d_0)^{-m}$, where d is the distance between transmitter and receiver, d_0 is the reference distance, and m is the path loss exponent [11]. The following simulations are based on $\sigma_h^2 = 1$, $d_0 = 1$km, and $m = 2.7$. The timing and carrier frequency offsets at $\mathbb{D}$, $\boldsymbol{\tau}^{[rd]}$ and $\boldsymbol{\nu}^{[sd]}$, respectively are assumed to be uniformly distributed over the range $(-0.5, 0.5)$. Based on the results in [3], [12], the timing offset estimation errors from $\mathbb{S} - \mathbb{R}$, $\epsilon_k^{[sr]}$, is assumed to follow a Gaussian distribution, i.e., $\epsilon_k^{[sr]} \sim \mathcal{N}(0, \sigma_\tau^2)$, where σ_τ^2 is set to the lower bound on the variance of timing offset estimation error in point-to-point systems [11, p. 328]. $d^{[sr]}$ and $d^{[rd]}$ are used to denote the $\mathbb{S}$-$\mathbb{R}$ and $\mathbb{R}$-$\mathbb{D}$ distances, respectively.

A. Estimation Performance

Specific channels are used to evaluate the MSE performance of the proposed estimators, i.e., $\mathbf{h} = [.279 - .9603j, .8837 + .4681j, -.343 + .732i, -.734 - .451i, 434 - .651i]^T$ and $\mathbf{f} = [.7820 + .6233j, .9474 - .3203j, -.2413 + .724i, .5141 - .893i, -.7141 - .393i]^T$ similar to [2], [4], [6]. First K elements of $\mathbf{h}$ and $\mathbf{f}$ vectors are used for K-relay network. Unless otherwise specified, $Q = 2$, $L_g = 10$, $d^{[sr]} = d^{[rd]} = 1$ km, and *quadrature phase-shift keying* (QPSK) modulation is used. Without loss of generality, MSE of the estimation parameters for the first relay is presented. Figs. 4(a), (b), and (c) show the CRLB and MSE for estimation of MTOs, MCFOs, and channel gains, respectively, with networks of 2 and 4 relays. It is shown that the MSEs of the proposed LS estimators are close to their CRLBs at mid-to-high SNRs. In comparison, the proposed SAGE estimator is close to the CRLB at mid-SNR values but exhibits some small performance degradation w.r.t. to the CRLB when estimating MCFOs, MTOs, and channel gains at high SNR due to the Taylor series approximations, which are used to linearize the LLF under consideration. In addition, Fig. 4(a) indicates that while estimating MTOs at high SNR, the MSEs of the proposed SAGE estimator exhibits an error floor. This error floor is due to the forward difference approximation used for evaluating the first and second order derivative of $b_i(\tau_k)$. However, as shown in Section IV-B, compared to the LS scheme, the SAGE estimator significantly reduces the computational complexity associated with estimating impairments in cooperative networks. Moreover, at low SNR, the proposed LS and SAGE estimators demonstrate poor performance due to the considerable timing offset estimation error from source to relays and the noise at the relays which is amplified and forwarded to the destination.

Fig. 5 and Fig. 6 presents the impact on the CRLB and MSE of SAGE algorithm for MCFOs estimation w.r.t. varying numbers of relays and TS lengths, respectively. Fig. 5 shows that estimation performance is close to the CRLB for different numbers of relays. It is worth mentioning that estimation performance has very minor degradation by increasing the number of relays. Fig. 6 shows that estimation performance improves by increasing the TS length. Further, it shows that MSE of SAGE estimator is away from the CRLB for $L = 16$, but gets close to the CRLB for $L \geq 32$ at SNR ≥ 20 dB.

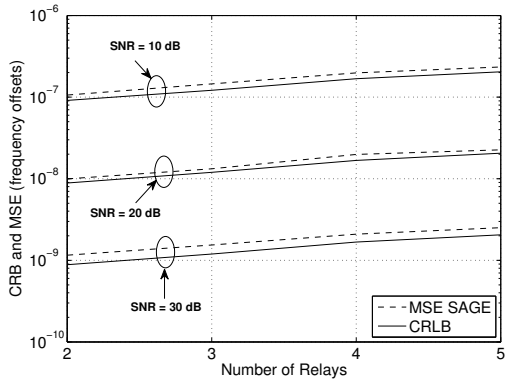

Fig. 5: MSE and CRLB of MCFOs estimation for different number of relays with $L = 64$.

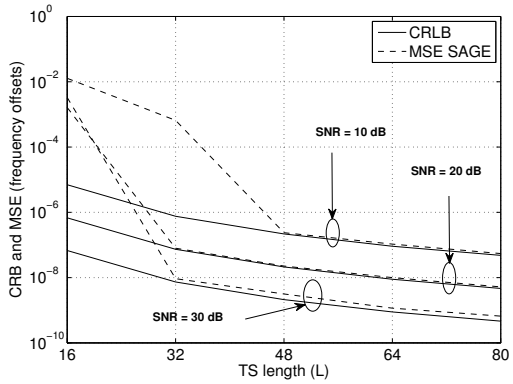

Fig. 6: MSE and CRLB of MCFOs estimation for different TS length with $K = 2$.

B. Convergence of SAGE Estimator

Table II shows the average number of iterations required by the SAGE algorithm to converge for different values of *signal-to-noise-ratio* (SNR). It can be observed from Table II that the proposed estimator converges after few iterations and is numerically stable.

TABLE II
AVERAGE NUMBER OF ITERATIONS REQUIRED FOR THE CONVERGENCE OF SAGE ALGORITHM.

Relays	SNR (dB)						
	0	5	10	15	20	25	30
$K = 2$	10.5	11.4	12.8	13.9	15.0	16.1	17.2
$K = 4$	12.4	14.1	15.4	16.7	17.8	19.0	20.4

C. Cooperative Performance

Fig. 7 shows the BER performance of a 2-relay cooperative network with BPSK and QPSK modulation schemes. The channel gains from source to relays and from relays to destination are modeled as *independent and identically distributed (i.i.d)* complex Gaussian random variables with $\mathcal{CN}(0, 1)$. We use *zero-forcing* (ZF) equalization, fixed gain relaying, synchronization overhead of 15%, and $Q = 4$ for the DTP. The results show that BER performance of SAGE estimator is close to the idealistic case of perfect impairment estimation i.e., *perfect estimation* (PE). Finally, we note that with the help of the proposed SAGE estimator, the BER of the overall cooperative network is below 10^{-3} for SNRs greater than 17dB and 23dB for BPSK and QPSK modulations, respectively.

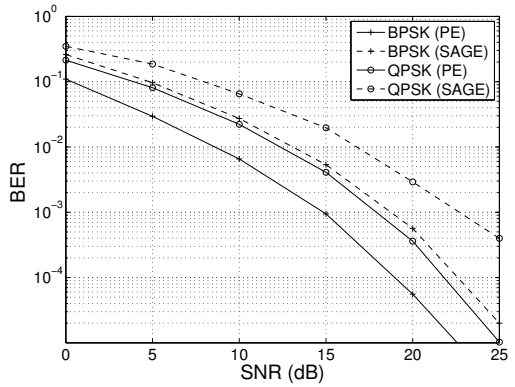

Fig. 7: BER performance of the cooperative system with 2 relays.

VI. CONCLUSIONS

In this paper a new transceiver design for achieving timing and frequency synchronization in AF cooperative networks is proposed. New closed-form CRLB expressions for the multiple parameter estimation problem are derived. Two estimation methods using LS and SAGE algorithms, are proposed for jointly estimating MCFOs, MTOs, and channel gains at the destination. In addition, it is established that at SNR of 20 dB for a 4-relay cooperative network, the execution time SAGE algorithm is approximately three orders of magnitude lower than an LS estimator. Simulation results show that the proposed estimators are close to the CRLB at mid-to-high SNRs for various number of relays and TS length ≥ 32.

REFERENCES

[1] A. Sendonaris, E. Erkip, and B. Aazhang, "User cooperative diversity - part I: system description; part II: implementation and performance analysis," *IEEE Trans. Commun.*, vol. 51, no. 11, pp. 1927–1948, Nov. 2003.

[2] H. Mehrpouyan and S. D. Blostein, "Bounds and algorithms for multiple frequency offset estimation in cooperative networks," *IEEE Trans. Wireless Commun.*, vol. 10, no. 4, pp. 1300–1311, Apr. 2011.

[3] X. Li, C. Xing, Y.-C. Wu, and S. C. Chan, "Timing estimation and resynchronization for amplify-and-forward communication systems," *IEEE Trans. Signal Process.*, vol. 58, no. 4, pp. 2218–2229, Apr. 2010.

[4] T. Pham, A. Nallanathan, and Y. Liang, "Joint channel and frequency offset estimation in distributed MIMO flat-fading channels," *IEEE Trans. Wireless Commun.*, vol. 7, no. 2, pp. 648–656, Feb. 2008.

[5] X. Li, Y. C. Wu, and E. Serpedin, "Timing synchronization in decode-and-forward cooperative communication systems." *IEEE Trans. Signal Process.*, vol. 57, no. 4, pp. 1444–1455, Apr. 2009.

[6] H. Mehrpouyan and S. D. Blostein, "Estimation, training, and effect of timing offsets in distributed cooperative networks," in *Proc. IEEE GLOBECOM*, Dec. 2010.

[7] Y. Tian, X. Lei, Y. Xiao, and S. Li, "ML synchronization algorithm and estimation bounds for cooperative systems," in *Proc IEEE Pacific Asia Conference on Circuits, Communications and Systems*, 2010.

[8] L. Dai, Z. Wang, J. Wang, and Z. Yang, "Joint channel estimation and time-frequency synchronization for uplink TDS-OFDMA systems," *IEEE Trans. Consum. Electron.*, vol. 56, no. 2, pp. 494–500, May 2010.

[9] J.-H. Lee and S.-C. Kim, "Time and frequency synchronization for OFDMA uplink system using the SAGE algorithm," *IEEE Trans. Wireless Commun.*, vol. 6, no. 4, pp. 1176–1181, Apr. 2007.

[10] A. A. Nasir, H. Mehrpouyan, S. D. Blostein, S. Durrani, and R. A. Kennedy, "Timing and carrier synchronization with channel estimation in multi-relay cooperative networks," *IEEE Trans. Signal Process.*, vol. 60, no. 2, Feb. 2012.

[11] H. Meyr, M. Moeneclaey, and S. A. Fechtel, *Digital Communication Receivers, Synchronization, Channel Estimation, and Signal Processing*, J. G. Proakis, Ed. Wiley Series in Telecom. and Signal Processing, 1998.

[12] S. M. Kay, *Fundamentals of Statistical Signal Processing: Estimation Theory*. NJ: Prentice Hall, 1993.

[13] T. A. Fessler and A. O. Hero, "Space-alternating generalized expectation maximization algorithm," *IEEE Trans. Signal Process.*, vol. 42, no. 10, pp. 2664–2677, Oct. 1994.

[14] N. Moller, "On Schoonhage's algorithm and subquadratic integer GCD computation," *Mathematics of Computation*, vol. 77, pp. 589–607, Jan. 2008.